LAKEHEAD UNIVERSITY

Department of Mechanical Engineering

EMEC-5671-SB: Renewable Energy for Mechanical Engineering Systems

Course Professor: Dr. Basel Ismail

Maximization of Solar PV & Wind Turbines Power Output using Modeling and Numerical Simulations – A Case Study of a Hypothetical Canadian Site

Group 23

Sheth Priyam – 1233198 (Seat No. – 70)

Suratwala Mihir – 1229926 (Seat No. – 73)

Date of Submission: 21st May, 2024

Table of Contents

Acknowledgement

We would like to express my deepest gratitude to my advisor, Dr. Basel Ismail, for his unwavering assistance, direction, and inspiration during our endeavour. His expertise and insightful feedback have been invaluable in shaping the direction and success of this study. We are particularly grateful for his patience and readiness to impart his extensive knowledge on renewable energy, which significantly contributed to the development of this research.

Dr. Ismail's commitment to excellence and his dedication to his students have been a source of inspiration. His constructive criticism and high standards have pushed me to perform at my best and have significantly enhanced the quality of my work. The numerous discussions and brainstorming sessions with him have not only improved my understanding of the subject matter but also broadened my perspective on research and its applications.

Thank you, Dr. Ismail, for being an outstanding mentor and for your unwavering support throughout this journey.

Statement of Student Code of Conduct – Academic Integrity (must be signed by the student):

As per the Lakehead University Student Code of Conduct – Academic Integrity, students are required to act ethically and with integrity in academic matters and demonstrate behaviours that support the university's academic values. In submitting this completed exam, I am therefore affirming the following statements to be true:

- I have completed this project without the assistance of anyone;
- With the exceptions of the course textbook, and Dr. Ismail's Class notes (EMEC-5671 course), and Google maps, I have NOT accessed any sources or materials (print, online, or otherwise) in the completion of this project;
- This project is protected by copyright. Reproduction or dissemination of this document or the contents or format of this document in any manner whatsoever (e.g., sharing the content with other students) is strictly prohibited. and;
- And, in accordance with Section III: Violations of this Academic Integrity Code, I understand that providing any false or misleading information, or by accessing any outside assistance, constitutes a breach of academic integrity as outlined in Lakehead University's Academic Integrity and Policies.

Student's Signature:

P.J.Sheth

M.P.Suratwala

Abstract

This project focuses on optimizing the power output of solar photovoltaic (PV) panels and wind turbines through modeling and numerical simulations, using a hypothetical site in Canada as a case study. The first component involves determining the unique optimum tilt angle β_{opt} for a solar PV panel to increase the collector's exposure to incoming solar radiation surface each month of the year, based on the site's coordinates. The PV panel's tilt angle ranges from 0 to 90 degrees in increments of 3 degrees. Using the Isotropic Model, the monthly average daily solar radiation incident on the tilted surface is estimated. Relevant calculations, including solar angles, clearness index, and beam geometric factor, are performed. Additionally, calculations to determine the monthly average hourly radiation are conducted to estimate hourly values for each month. This analysis ensures that the solar energy system operates at peak efficiency throughout the year by adjusting the tilt angle according to the sun's changing position.

The second component aims to estimate the available wind energy at the same site to evaluate the viability of installing a horizontal-axis, two-blade, high-speed wind turbine. This involves analyzing wind speed data to determine the wind energy generated based on the monthly wind data. Utilizing these values, calculations are conducted to determine the actual producible wind energy using the power coefficient available for the two-blade high-speed wind turbine. This estimation provides insight into the potential power generation of the wind turbine throughout the year at the specified site coordinates. Conducting detailed research, we identify a wind turbine model that fits the site-specific conditions and energy requirements. The selected turbine is then evaluated using various metrics to assess its contribution to the site's renewable energy portfolio.

Through these two components, the project aims to offer a thorough examination of the renewable energy potential at the hypothetical site, offering insights into the optimal deployment of solar and wind energy systems.

List of Figures

List of Tables

Nomenclature

PV – Photovoltaics

Lat. – Latitude

Long. – Longitude

(β_{opt}) – Optimal inclination angle

($\bar{H}$) – Monthly average daily solar insolation incident on a horizontal surface

($\overline{\rho_g}$) – Ground reflectance (albedo)

($\bar{\eta}$) – Mean days for a month

(ϕ) – Site coordinates

(δ) – Declination angle

(ω_s) – Sunset hour angle

($\overline{H_o}$) – Monthly average daily extra-terrestrial radiation

($\overline{K_T}$) – Clearness index

($\frac{\overline{H_d}}{\bar{H}}$) – Monthly average daily diffuse to total radiation on a horizontal surface

($\overline{R_b}$) – Beam geometric factor

($\overline{H_T}$) – Monthly average daily radiation incident on the tilted PV surface

$(\bar{I}_T)_{opt}$ – Monthly average hourly solar radiation

($\overline{Ta}$) – Monthly average air temperature

($\bar{P}_a$) – Monthly average atmospheric pressure

($\overline{v_\omega}$) – Monthly average wind speed

($\frac{P_{t,w}}{A}$) – Available wind energy density

($P_{t,w}$) – Available wind energy

(F_{max}) – Maximum axial thrust

($v_{w,e}$) – Exit wind velocity

($v_{w,i}$) – Incoming wind velocity

(v_T) – Total wind velocity

($P_{t,act}$) – Actual producible wind energy

(ω_{rpm}) – Operational speed

(τ) – Torque

Introduction

Renewable energy stands as the most effective means of energy generation, playing a pivotal role in curbing carbon emissions and stabilizing Earth's temperature levels. Among these renewable sources, solar and wind systems emerge as primary contenders for sustainable energy production. This project is primarily dedicated to optimizing the tilt angle of solar photovoltaic (PV) panels to maximize utilizable solar radiation and evaluating the available wind energy output for specified site coordinates, while also exploring the application of a commercial wind turbine.

The chosen location for analysis, identified as Alma, Quebec (48.55 N (Lat.) and 71.65 W (Long.)), offers a strategic setting situated on the southeast coast of Lac Saint-Jean, where it converges with the Saguenay River [3]. Alma, the second largest city in the Saguenay-Lac-Saint-Jean region, boasts a population that has steadily grown from around 29,998 in 2006 to 30,915 in 2021 [3]. Alma has a humid continental climate with warm summers and plenty of precipitation, making it an ideal location for renewable energy development [3]. The district's yearly temperature is 7.4ºC (45.32ºF) and it is 5.31% higher than Canada's averages. Alma typically receives about 38.93 millimetres (1.53 inches) of precipitation and has 44.18 rainy days (12.1% of the time) annually.

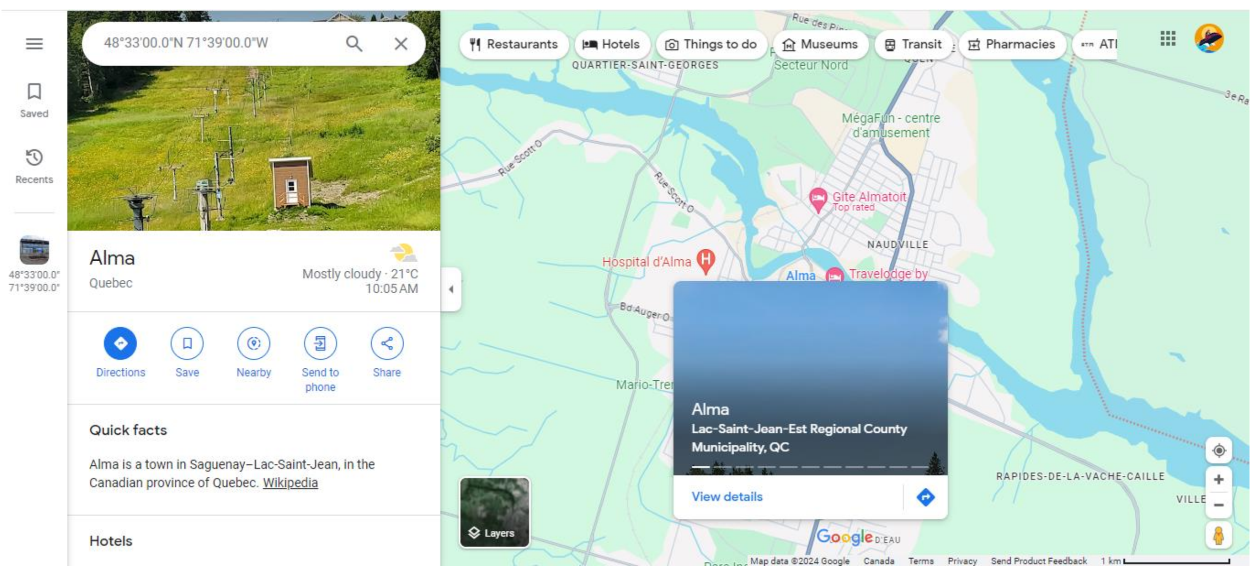

Figure 1: Map of Alma Quebec

Given the significance of tilt angle optimization in solar PV systems, this project aims to determine the ideal inclination at which a PV module should be sloped from the horizontal. This parameter profoundly influences system performance, as variations in tilt angle directly impact the amount of incident solar radiation received and utilized by the PV system. Optimizing the tilt angle not only maximizes power production throughout the year but also reduces the required PV array area, thus mitigating system costs.

In parallel, the project delves into the assessment of wind energy potential, crucial for determining the feasibility of deploying a horizontal-axis two-blade, high-speed wind turbine at the specified site coordinates. By estimating available wind energy and projecting annual power generation from the turbine, the project seeks to ascertain the viability of turbine installation at the designated location. This comprehensive analysis encompasses considerations of optimal wind speeds necessary for effective power generation from the turbine system.

By addressing both solar and wind energy components, this project endeavours to offer insights into the renewable energy prospects at the Alma site, contributing to the broader discourse on sustainable energy solutions and fostering informed decision-making in energy infrastructure development.

Objective

Part A: The objective of this study is to conduct a comprehensive analysis of solar radiation and its effects on photovoltaic (PV) panel performance. This involves calculating solar angles, such as the sunset hour angle and declination angle, based on the average day of each month throughout the year. Subsequently, solar radiation parameters including global horizontal irradiance, clearness index, and beam radiation geometric factor will be estimated. The analysis will further extend to calculate the radiation incident on tilted PV surfaces considering the optimal tilt angle. Additionally, contributions from beam, diffuse, and ground-reflected radiation will be quantified and compared. The yearly averaged tilt angle will also be determined to assess overall PV panel orientation. Furthermore, monthly average hourly solar radiation will be calculated for daylight hours, accounting for symmetrical conditions around noontime, using the optimal tilt angle for each month. These calculations aim to provide insights into solar energy availability and inform optimal PV panel positioning for enhanced energy capture.

Part B: The objective of this study is to analyze wind energy potential and assess the feasibility of installing a horizontal-axis two-blade, high-speed turbine at specified site coordinates. This involves calculating monthly and annual wind energy density, estimating turbine-received wind energy, and determining producible wind energy based on the Betz limit. Additionally, computations will be made for maximum axial thrust, actual producible wind energy using performance curves, and operational speed and torque. Furthermore, research will be conducted to select a commercial wind turbine, presenting a related case study, turbine specifications, and discussing the rationale behind the selection, supported by a detailed design diagram.

Task Division

Task	Question List	Priyam Sheth	Mihir Suratwala
Location Research	-	50%	50%
Part A	1	-	100%
	2	-	100%
	3	-	100%
	4	-	100%
	5	100%	-
	6	100%	-
	7	100%	-
	8	100%	-
	9	70%	30%
	10	50%	50%
	Excel	70%	30%
Part B	1	-	100%
	2	-	100%
	3	-	100%
	4	100%	-
	5	70%	30%
	6	100%	-
	7	50%	50%
	Excel	50%	50%
Report	-	50%	50%
Conclusion	-	50%	50%

Simulation Procedure

Part A: Basically, we were given the site coordinates (48.55 N (Lat.) and 71.65 W (Long.)), monthly average daily solar insolation incident on a horizontal surface $\overline{H}(\frac{kWh}{m2})$, monthly average ground reflectance (albedo) $\overline{\rho_g}$ and mean days for a month ($\overline{\eta}$).

Month	Jan	Feb	Mar	Apr	May	Jun	Jul	Aug	Sep	Oct	Nov	Dec
Hbar (kWh/m2)	1.44	2.35	3.57	4.65	5.07	5.46	4.97	4.46	3.23	1.95	1.31	1.11
Hbar (MJ/m2)	5.184	8.46	12.852	16.74	18.252	19.656	17.892	16.056	11.628	7.02	4.716	3.996
Pgbar	0.31	0.28	0.3	0.24	0.09	0.1	0.1	0.09	0.1	0.09	0.21	0.28
nbar	17	47	75	105	135	162	198	228	258	288	318	344

Figure 2: Given Solar Energy Data

As we know the site coordinates (ϕ) and mean days for a month ($\overline{\eta}$), we calculate the declination angle (δ) and sunset hour angle (ω_s) using the equation given in Appendix I as (4) and (5). Keeping the values of declination angle (δ) and sunset hour angle (ω_s), using the equation given in Appendix I as (6), we can calculate the value of monthly average daily extra-terrestrial radiation ($\overline{H_o}$) for each month. Using the value of monthly average daily extra-terrestrial radiation ($\overline{H_o}$) for each month and monthly average daily solar insolation incident on a horizontal surface ($\overline{H}$), we can calculate the value of clearness index ($\overline{K_T}$). As per the values of ($\overline{K_T}$) and (ω_s), we need to check the condition, and based on the value, either equation (2) or (3) can be used, as given in Appendix I. Based on that, we can calculate the value of the monthly average daily diffuse to total radiation on a horizontal surface ($\frac{\overline{H_d}}{\overline{H}}$). On the other side, taking the values of declination angle (δ), sunset angle (ω_s), inclination (tilt) angle (β) and latitude (ϕ), we can obtain the value of beam geometric factor ($\overline{R_b}$). By changing the values of inclination (tilt) angle (β), we can obtain the different values of beam geometric factor ($\overline{R_b}$) using equations (7) and (8) given in Appendix I. As per the given project guidelines, we can vary the inclination (tilt) angle (β) from 0 to 90 degrees. Now, we have all the values that are required for the calculation of the monthly average daily radiation incident on the tilted PV surface ($\overline{H_T}$). Using these values, we can find the maximum value of ($\overline{H_T}$) at a particular inclination angle (β) and this inclination angle (β) will be the optimal inclination angle (β_{opt}) for that month. Using the value of ($\overline{H_T}$), we can also find the value of beam ($\overline{H_{T_b}}$), sky diffuse ($\overline{H_{T_d}}$) and ground reflectance ($\overline{H_{T_g}}$) for each month considering the optimal inclination angle (β_{opt}). For the calculation of the monthly average hourly solar radiation $(\overline{I_T})_{\text{opt}}$, we will be using the equation (10) from Appendix I. As we have all the values, we can calculate the values of $r_t, r_d, a, b, \omega, N\ and\ R_b$ using the equation given in Appendix I as (11), (12-a), (12-b), (12-c), (13), (14) and (15). For the calculation of daylight hours (N), will be consider the given time as solar time and take the midpoint value of the hour pair. Also, while determining the number of daylight hours, consider the symmetrical hours around noon to avoid getting negative values of $(\overline{I_T})_{opt}$.

Part B: Basically, we were given data such as monthly average air temperature ($\overline{Ta}$), monthly average atmospheric pressure ($\overline{P_a}$), gas constant (R), radius of turbine (r), elevation (H) and monthly average wind speed ($\overline{v_\omega}$).

Month	TaBar (C)	PaBar (kPa)	VwBar (m/s)	TaBar (K)	PaBar (Pa)
January	-17.7	96.6	4.57	255.3	96600
February	-15.3	96.7	4.5	257.7	96700
March	-8.94	96.7	4.61	264.06	96700
April	-0.18	96.7	4.44	272.82	96700
May	8.71	96.7	4.58	281.71	96700
June	14.7	96.6	4.44	287.7	96600
July	17.2	96.7	4.09	290.2	96700
August	16	96.9	4.11	289	96900
September	10.8	96.9	4.58	283.8	96900
October	3.42	96.9	4.57	276.42	96900
November	-4.68	96.7	4.54	268.32	96700
December	-12.9	96.7	4.53	260.1	96700

Figure 3: Given Wind Energy Data

Using these values, we were able to calculate the available wind energy density ($\frac{P_{t,w}}{A}$) using equation (B-1) mentioned in the sample calculation of this report. As per the project guidelines, we need to consider the same average wind speed for the entire month. So, the number of hours in each month can be calculated as the number of days in a month multiplied by the number of hours per day. By using the number of hours in a month and wind energy density ($\frac{P_{t,w}}{A}$), we obtained the available wind energy ($P_{t,w}$) received by the turbine for each month. Considering the Betz limit, the maximum efficiency of the wind turbine will be 59.26%, or (16/27). Using the Betz limit, we calculated the value of producible wind energy using the equation (B-2) mentioned in the sample calculation of this report. To calculate the maximum axial thrust (F_{max}), we need to calculate the exit wind velocity ($v_{w,e}$) and total wind velocity (v_T). For that, we will consider the exit wind velocity ($v_{w,e}$) as the optimal exit wind velocity (v_{opt}), which can be obtained using the equation (B-3) mentioned in the sample calculation of this report. The total wind velocity (v_T) can be obtained using the equation (B-4) mentioned in the sample calculation of this report. Now that we have all the required values, using equation (B-5) mentioned in the sample calculation of this report, we can calculate the value of the maximum axial thrust (F_{max}) acting on the turbine bearings. Furthermore, we need to find the actual producible wind energy. For that, we need to use Figure k-1[1] and Excel to find the relationship between the power coefficient (c_P) and advanced ratio (λ). This relationship will help to find the value of the power coefficient (c_P) and advanced ratio (λ). Using these values, we can easily calculate the value of actual producible wind energy ($P_{t,act}$). By using the relationship, we can also find the value of operational speed (ω_{rpm}) and torque (τ) for each month in the turbine by using the equations (B-6) and (B-7) mentioned in the sample calculation of this report. On the basis of this study, we need to do research and find out the wind turbine that can fit this application.

Sample Calculations

Part A:

Given Data:

$\beta = 3^o$, $\gamma = 0^o$

$\overline{\rho g} = 0.31$ (For the month of Jan)

$\emptyset = 48.55^o$, $\bar{n} = 17$ (For the month of Jan)

$\overline{H} = 1044$ kWh/m^2 (For the month of Jan)

$= 3.6 \times 1.44$

$= 5.184$ MJ/m^2

1.) Calculate solar angles: Declination angle (δ) and Sunset hour angle (ω_s)

$$\delta = 23.45^o \sin\left(360\left[\frac{284+\bar{n}}{365}\right]\right)$$

$$= 23.45^o \sin\left(360\left[\frac{284+17}{365}\right]\right)$$

$$= 23.45^o \sin[296.87]$$

$$= -20.91$$

$$\omega_s = \cos^{-1}(-\tan\emptyset \tan\delta)$$

$$= \cos^{-1}(-\tan(48.55) \text{ X } \tan(-20.91))$$

$$= \cos^{-1}(0.4326)$$

$$\omega_s = 64.3670$$

2.) Calculate $\overline{Ho}$ (MJ/m^2)

$$\overline{Ho} = \frac{24 \times 3600 \times 1367}{\pi}\left(1 + 0.033\cos\left(\frac{360 \times \bar{n}}{365}\right)\right) \times \left(\cos\emptyset \cos\delta \sin\omega_s + \frac{\pi\omega s}{180}\sin\emptyset \sin\delta\right)$$

$$\overline{Ho} = \frac{24 \times 3600 \times 1367}{\pi}\left(1 + 0.033\cos\left(\frac{360 \times 17}{365}\right)\right) \times \left(\cos(48.55^o)\cos(-20.91^o)\sin(64.36^o) + \frac{\pi \times 64.36}{180}\sin(48.55^o)\sin(-20.91^o)\right)$$

$$\overline{Ho} = 37595198.69\,(1.0315) \times (0.5575 + 1.1232(-0.2675))$$

$$\overline{Ho} = 9967050.15 \text{ J/m}^2$$

$\overline{Ho}$ = 9.9670 MJ/m^2

3.) Calculate monthly average daily clearness index ($\overline{K_T}$)

$$\overline{K_T} = \frac{\overline{H}}{\overline{Ho}} = \frac{5.184}{9.9670} = 0.5201$$

ω_s = 64.3670

$\omega_s \leq 81.4^o \quad 0.3 \leq \overline{KT} \leq 0.8$

4.) Estimate the fraction of monthly average daily diffuse to total radiation on a horizontal surface ($\frac{\overline{Hd}}{\overline{H}}$).

$$\frac{\overline{Hd}}{\overline{H}} = 1.391 - 3.560\ \overline{KT} + 4.189\ \overline{KT}^2 - 2.137\ \overline{KT}^3$$

$$= 1.391 - 3.560\ (0.5201) + 4.189(0.5201)^2 - 2.137(0.5201)^3$$

$$= 0.3719$$

5.) Calculate the monthly average daily geometric factor of beam radiation $\overline{Rb}$.

ω_s = 64.3670, $\beta = 3^o$, $\emptyset = 48.55^o$, $\delta = (-20.91^o)$

$$\overline{Rb} = \frac{\cos(\emptyset-\beta)\ cos\delta\ sin\omega_s' + \frac{\pi}{180}\ \omega_s' \sin(\emptyset-\beta)\ sin\delta}{\cos(\emptyset)\ cos\delta\ sin\omega_s + \frac{\pi}{180}\ \omega_s \sin(\beta)\ sin\delta}$$

$$\omega_s' = \min\begin{bmatrix} cos^{-1}(-tan\emptyset\ tan\delta) \\ cos^{-1}(-\tan(\emptyset-\beta)\ tan\delta) \end{bmatrix}$$

$$= \min\begin{bmatrix} cos^{-1}(-tan 48.55)\tan(-20.91) \\ cos^{-1}(-\tan(45.55)\tan(-20.91) \end{bmatrix}$$

$$\omega_s' = \min\begin{bmatrix} 64.3670 \\ 67.0785 \end{bmatrix}$$

ω_s' = 64.3670

$$\overline{Rb} = \frac{\cos(45.55)\cos(-20.91)\sin(64.3670) + \frac{\pi}{180}(64.3670)\sin(45.55)\sin(-20.91)}{\cos(48.55)\cos(-20.91)\sin(64.3670) + \frac{\pi}{180}(64.3670)\ \sin(48.55)\sin(-20.91)}$$

$$\overline{Rb} = \frac{0.5897 + (-0.2862)}{0.5575 + (-0.3005)} = \frac{0.3035}{0.2570} = 1.1809$$

6.) Estimate the monthly average daily radiation incident on the tilted PV surface ($\overline{H_T}$)

$$\overline{H_T} = \overline{H}\ (1 - \frac{\overline{H_d}}{\overline{H}})\ \overline{R_d} + \overline{H_d}\ (\frac{1+cos\beta}{2}) + \overline{H}\ \overline{\rho g}\ (\frac{1-cos\beta}{2})$$

$= 5.184\ (1 - 0.3719)\ 1.1809 + 1.927\ (\frac{1+\cos 3}{2}) + 5.184 \times 0.31 \times (\frac{1+\cos 3}{2})$

$= 3.8450 + 1.9256 + 1.1011 \times 10^{-3}$

$\overline{H_T} = 5.7716$

7.) Calculate the monthly average daily contributions for beam ($\overline{H_{T_b}}$), sky diffuse ($\overline{H_{T_d}}$), and ground reflectance ($\overline{H_{T_g}}$) for each month considering the optimum tilt angle.

Table 1: Monthly average daily contributions for beam, sky diffuse, and ground reflectance

$\overline{H_{T_b}}$	$\overline{H_{T_b}}/\overline{H_T} \times 100$	$\frac{3.8450}{5.7716} X\ 100$	66.61%
$\overline{H_{T_d}}$	$\overline{H_{T_d}}/\overline{H_T} \times 100$	$\frac{1.9256}{5.7716} X\ 100$	33.36%
$\overline{H_{T_g}}$	$\overline{H_{T_g}}/\overline{H_T} \times 100$	$\frac{0.001011}{5.7716} X\ 100$	0.0017%

8.) Calculate $(\overline{R})_{max}$ to optimal tilt angle for each month.

$$(\overline{R})_{max} = \frac{(\overline{H_T})\ max}{\overline{H}} \quad \text{(For each month)}$$

Table 2: $(\overline{R})_{max}$ value for each month

Month	Jan	Feb	Mar	Apr	May	Jun	Jul	Aug	Sep	Oct	Nov	Dec
$(\overline{R})_{max}$	2.630 45	1.920 65	1.377 45	1.100 41	1.013 06	1.001 04	1.004 38	1.042 50	1.165 92	1.459 31	2.090 25	2.747 30

9.) Calculate $(\beta_{opt})_{year}$

$$(\overline{\beta_{opt}})_{year} = \frac{\sum_{Jan}^{Dec}(\beta_{opt})}{12} = 41.5^0$$

10.)

$$\overline{I_T} = \overline{K_T}\ \overline{Ho}\ \left[\left(rt - \frac{\overline{Ho}}{\overline{H}}\right) Rb + \frac{\overline{Hd}}{\overline{H}}\ rd\ \left(\frac{1+\cos\beta}{2}\right) + \overline{\rho g}\ rt\ (\frac{1-\cos\beta}{2})\right]$$

a.) $r_d = (\frac{\pi}{24}) \left[\frac{\cos\omega - \cos\omega_S}{\sin\omega_S - \frac{\pi\omega_S}{180}\cos\omega_S}\right]$

ω = 15 (ST – 12) = 15(10.5 -12) = 15(-1.5) = -22.5

$r_d = (\frac{\pi}{24}) \left[\frac{\cos(-22.5) - \cos(64.3670)}{\sin(64.3670) - \frac{\pi(64.3670)}{180}\cos(64.3670)}\right] = (\frac{\pi}{24}) \left[\frac{0.4912}{0.4156}\right]$

$r_d = 0.1547$

b.) $r_t = (\frac{\pi}{24})\ (a + b\cos\omega) \left[\frac{\cos\omega - \cos\omega_S}{\sin\omega_S - \frac{\pi\omega_S}{180}\cos\omega_S}\right]$

$a = 0.409 + 0.5016 \sin(\omega_s - 60^o)$

$a = 0.409 + 0.5016 \sin(64.3670 - 60^o)$

$a = 0.4471$

$b = 0.6609 - 0.4767 \sin(\omega_s - 60^o)$

$b = 0.6609 - 0.4767 \sin(64.3670 - 60^o)$

$b = 0.6246$

$r_t = (a + b\cos\omega)\ r_d$

$= [(0.4471 + 0.6246 \cos(-22.5)]\ (0.1547)$

$r_t = 0.1584$

c.) $R_b = \frac{\cos(48.55-3)\cos(-20.91)\cos(-22.5)+\sin(48.55-3)\sin(-20.91)}{\cos(48.55-3)\cos(-20.91)\cos(-22.5)+\sin(48.55-3)\sin(-20.91)}$

$R_b = \frac{0.6043+(-0.2547)}{0.5712+(-0.2675)} = \frac{0.3496}{0.3037} = 1.1511$

$$\overline{I_T} = \overline{K_T}\ \overline{Ho} \left[\left(rt - \frac{\overline{Ho}}{\overline{H}}\ rd\right) Rb + \frac{\overline{Hd}}{\overline{H}}\ rd \left(\frac{1+\cos\beta}{2}\right) + \overline{\rho g}\ rt \left(\frac{1-\cos\beta}{2}\right)\right]$$

$\overline{I_T}$ = (0.5201) (9.9670) $\left[\{(0.1584) - (0.3719)\ (0.1547)\}\ (1.1511) + (0.3719)\ (0.1547)\ \left(\frac{1+\cos 3}{2}\right) + (0.31)\ (0.1584)\ \left(\frac{1-\cos 3}{2}\right)\right]$

$\overline{I_T}$ = 5.1838 × 0.1735 = 0.8995

Table 3: Average value of inclination angle for four seasons

Season	**Dec-Feb**	**Mar-May**	**Jun-Aug**	**Sept-Nov**
$\boldsymbol{(\beta_{avg})_{season}}$	71	31	11	53

For the calculation of Daylight Hours, $N = \frac{2}{15}\omega_s$

Table 4: Daylight hours for each month

Month	**Jan**	**Feb**	**Mar**	**Apr**	**May**	**Jun**	**Jul**	**Aug**	**Sep**	**Oct**	**Nov**	**Dec**
N (Daylight Hours)	8	10	12	12	14	16	14	14	12	10	8	8

Part B:

Given Data:

R = 0.287 KJ/Kg K

= 287 J/Kg K

D (Diameter of Turbine) = 10 m

R (Radius of Turbine) = D/2 = 5 m

H (Elevation) = 50 m

$\overline{V_w}$ = 4.57 m/s (For the month of Jan)

1.) Calculate Average Wind Energy Density (kWh/m^2)

$\overline{T_a}$ = -17.7^o C (Given for Jan Month)

$\overline{T_\alpha}$ = 273 + (-17.7) = 255.3^o K

$\overline{P_\alpha}$ = 96.6 KPa = 96.6 × 10^3 Pa

Hours = 31 x 24 = 744 (For the month of Jan)

$\rho = \frac{P}{R\,T_a} = \frac{96.6 \times 10^3}{287 \times 255.3}$ = 1.3183

$(\frac{P_t,\omega}{A}) = \frac{1}{2}\,\rho v_{\omega,i}^3$ **--- Equation (B-1)**

$(\frac{P_t,\omega}{A}) = \frac{1}{2}$ × 1.3187 × $(4.57)^3$ = 62.911 W/m^2 = 0.0629 kW/m^2

= 0.0629 × 744 kWh/m^2 = 46.7976 kWh/m^2

Annual Wind Energy Density = 483.2042701 kWh/m^2 (From Excel Calculation)

2.) Calculate Wind Energy (kWh) for turbine

$(\frac{P_t,\omega}{A})$ = 46.7976

A = πr^2

= $\pi \times (5)^2$

= 78.5398 m^2

$P_{t,\,\omega}$ = 46.7976 × A

= 46.7976 × 78.5398

= 3675.4749 kWh

$P_{t,\,\omega}$ = 3.6754 MWh

Annual Wind Energy = 37950.77463 kWh (From Excel Calculation)

3.) Calculate the Ideal (Betz limit) Producible Wind Energy ($P_{T,\,max}$)

$P_{T,\,max} = \frac{16}{27} \times P_{t,\,\omega}$ **--- Equation (B-2)**

$P_{T,\,max} = \frac{16}{27} \times 3.6754 = 2.1780$ MWh

4.) Calculate Monthly Average Maximum Axial Thrust (F_{max})

$F_{max} = \rho v_T A\left(v_{w,i} - v_{\omega,e}\right)$

$\rho = 1.3183$

A = 78.5398

$v_T = \frac{1}{2}(v_{w,i} + v_{\omega,e})$

For $P_{T\,max} \rightarrow (v_{\omega,e})_{opt} = \frac{1}{3} v_{w,i}$ **--- Equation (B-3)**

$(v_{\omega,e})_{opt} = \frac{1}{3}(4.57) = 1.5233$ m/s

$v_T = \frac{1}{2}(v_{\omega,i} + v_{\omega e})$ **---Equation (B-4)**

$v_T = \frac{1}{2}(4.57 + 1.5233)$

$v_T = 3.0466$ m/s

$F_{max} = \rho v_T A\left(v_{w,i} - v_{\omega,e}\right)$ **---Equation (B-5)**

$F_{max} = (1.3183)\,(3.0466)\,(78.5398)\,(\frac{2}{3})\,(4.57)$

= 96.0465 N

= 0.961 kN

5.) Using the performance curve of two-blade-high-speed wind turbine given as Figure k-1 [1], obtained the function from the Excel using the Trendline. So, the function obtained is as follows:

$y = -(0.0066)x^2 + (0.1424)x - 0.2993$

For the finding the maximum value we need to differentiate the above equation and equate with zero. Here y represents as Cp and x represents as λ:

$$\frac{dy}{dx} = -(0.0066)(2x) + (0.1424) = 0$$

$$x = 10.7878$$

By using the value of x in the above function, we can calculate the value of y as:

$$\mathrm{y} = 0.4687$$

The Actual Producible Wind Energy can be calculated as:

$$\mathrm{P_{act}} = \eta_{\mathrm{act}} \times \mathrm{P_{t,\omega}} = 0.4687 \times 3.6754 = 1.7226 \text{ MWh}$$

Annual Actual Producible Wind Energy = 17787.52807 kWh (From Excel Calculation)

6.) Calculate the monthly average actual operational speed (RPM) and Torque

$$\omega_{\mathrm{rad}} = \frac{\lambda \times \mathrm{v}_{\omega,\mathrm{i}}}{\mathrm{R}} = \frac{10.7878 \times 4.57}{5} = 9.8529\ rad/sec$$ **-- Operational Speed**

$$\omega_{rpm} = \left(\frac{60}{2\pi}\right) \times \omega_{\mathrm{rad}} = \left(\frac{60}{2\pi}\right) \times 9.8529 = 94.1361\ rpm$$

$$\tau = \frac{P_{act}}{\omega_{\mathrm{rad}}} = \frac{1.7226}{9.8529} = 174.8317\ kNm$$ **-- Torque**

7.) Selection of Wind Turbine for Alma, Quebec: Eocycle EOX S-16

Case Study: Eocycle EOX S-16, Alma, Quebec

Location Overview

Alma is located in the Saguenay–Lac-Saint-Jean region of Quebec, Canada, with coordinates 48.55°N latitude and 71.65°W longitude. The region experiences a humid continental climate with warm summers and cold winters, making it suitable for both solar and wind energy generation. The average wind speed in Alma is between 4-5 m/s, which is ideal for small to mid-sized wind turbines.

Load Requirement and Application

For a residential or small commercial application in Alma, Quebec, the energy requirements are typically around 15-20 MWh annually [2]. This makes the EOX S-16, with its annual energy production capability, a suitable candidate. The turbine will be used to provide renewable energy for a small business or residential complex, reducing dependency on grid power and lowering carbon emissions.

Wind Turbine Selection: Eocycle EOX S-16

Specifications

Rated Power: 20 kW to 30kW depending on version

Annual Energy Production: 40-70 MWh at wind speeds of 4-5 m/s

Cut-in Wind Speed: 2.75 m/s

Rated Wind Speed: 7.5 m/s (Average Annual Wind Speed)

Cut-out Wind Speed: 20 m/s

Rotor Diameter: 15.8 meters

Hub Height: 16.8 or 23.8

Blade Length: 7.6 m

Design Diagram

Below is a simplified design diagram of the Eocycle EOX S-16 wind turbine:

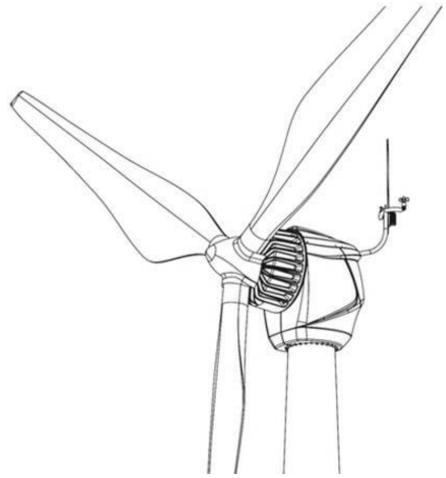

Figure 4[2]: Design of Eocycle EOX S-16

Detailed Discussion

Performance and Suitability

The Eocycle EOX S-16 is designed for moderate wind speeds, making it suitable for Alma, Quebec, where the average wind speed is 4-5 m/s. The turbine's ability to start generating power at low wind speeds (cut-in at 2.5 m/s) ensures consistent energy production throughout the year. The operating temperature of the turbine is -20^{o}C to 40^{o}C which makes it suitable for our application as the temperature varies for Alma, Quebec is between -20^{o}C to 25^{o}C [2].

Energy Production Analysis

Based on the site's average wind speed, the EOX S-16 is expected to produce between 40 and 70 MWh annually [2]. This output is well above the required 17.78 MWh, ensuring that the energy needs are comfortably met and excess energy can be stored or sold back to the grid.

Load Matching

For a residential complex or small business in Alma, the EOX S-16 can provide a significant portion of the required energy, leading to reduced electricity bills and a lower carbon footprint. The consistent axial thrust and efficiency in handling variable wind conditions also ensure reliable operation and maintenance predictability. In EOX S-16, have a very few moving parts and also it has no gearbox so, it will reduce the periodic maintenance of the system. It has a good design life of 30 years without any major component replacement.

Economic and Environmental Impact

The installation of the EOX S-16 wind turbine will significantly cut down on electricity costs, providing a return on investment within a few years. Environmentally, it contributes to reducing greenhouse gas emissions, aligning with Quebec’s renewable energy goals.

Conclusion

The EOX S-16 wind turbine is an ideal choice for the given site in Alma, Quebec, based on its specifications, performance, and ability to meet the local energy requirements. Its robust design and efficiency in moderate wind conditions make it a reliable source of renewable energy. Detailed analysis and site-specific data support the feasibility and benefits of this installation, ensuring long-term sustainability and economic advantages.

For more such details, we had attached the specifications document at the end of this report.

Discussion

Part A: The graphs shown below indicate that these factors vary by month throughout the year, potentially influencing the efficiency of solar energy collection.

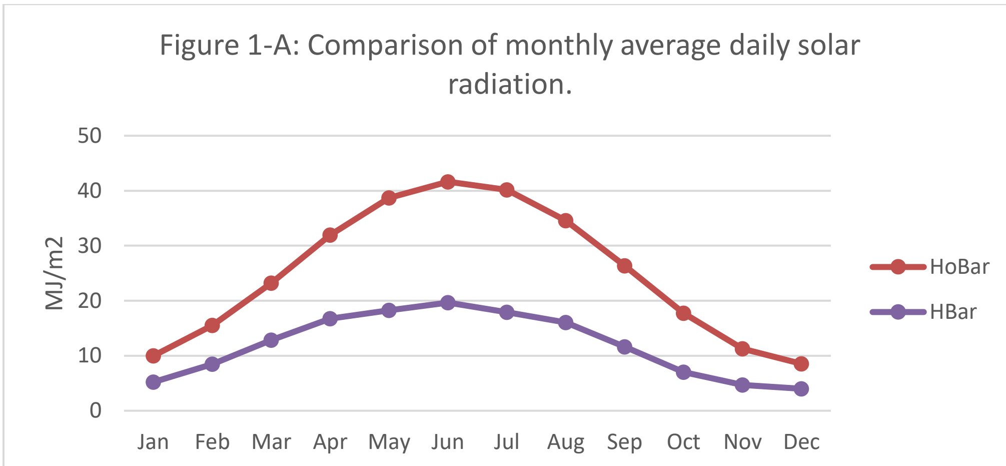

Figure 1-A: Comparison of monthly average daily solar radiation.

Both lines show a clear seasonal pattern, with solar radiation peaking in the summer months and dropping during the winter months. The $\overline{H_0}$ consistently shows higher levels of solar radiation throughout the year compared to the $\overline{H}$ with the maximum radiation occurring in June.

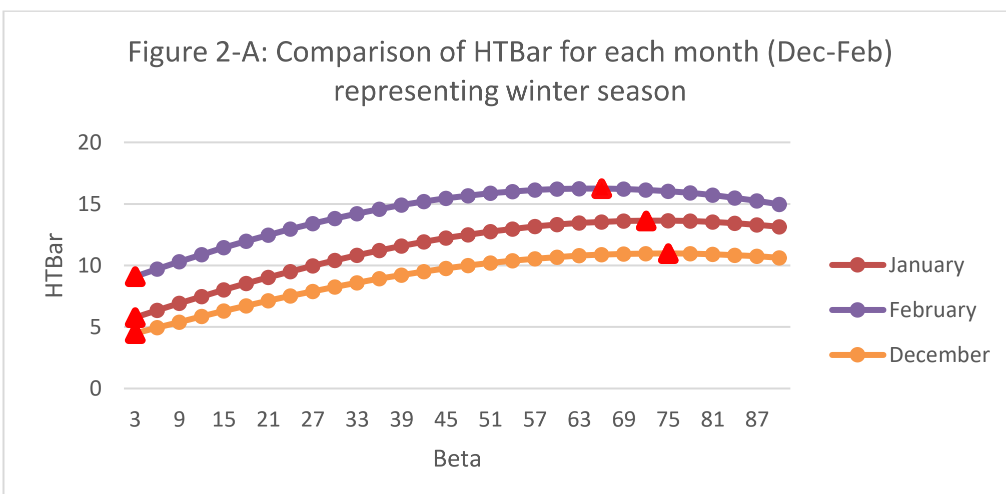

Figure 2-A: Comparison of $\overline{H_T}$ for each month (Dec-Feb) representing winter season

The graph shows that $\overline{H_T}$ generally increases as the inclination angle β increases for each of the winter months. The lines for December, January, and February run parallel, indicating a consistent monthly increase in $\overline{H_T}$ during the winter season. This suggests that the inclination angle β has a positive correlation with $\overline{H_T}$, and this relationship is consistent across the three winter months represented.

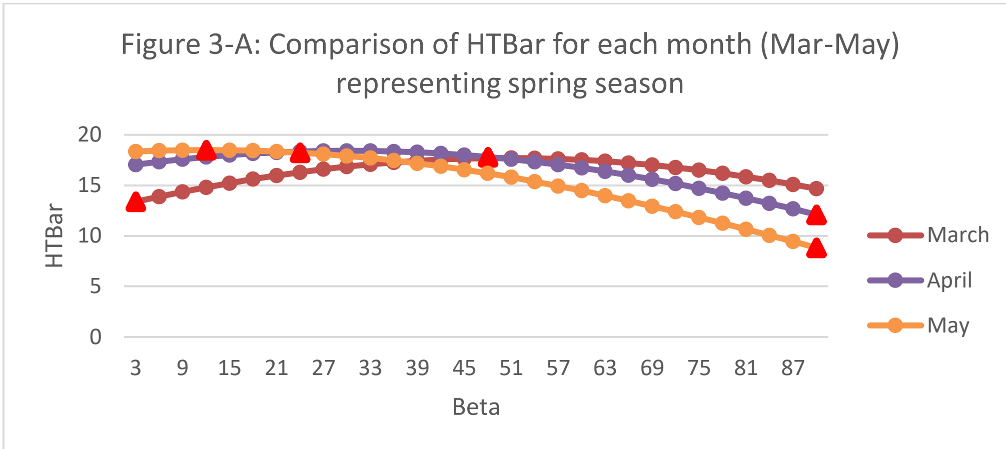

Figure 3-A: Comparison of $\overline{H_T}$ for each month (Mar-May) representing spring season

The graph shows a downward trend in $\overline{H_T}$ as the inclination angle β increases for the months of March, April, and May. As, march starts with the lowest $\overline{H_T}$ values and peaks as the inclination angle β increases, attaining the highest value at the end. Whereas in April and May, dropping in $\overline{H_T}$ values are observed as the value of inclination angle β increases. This suggests that during the spring season, as the inclination angle β increases, the $\overline{H_T}$ value decreases consistently across the months. So, we can say that on approaching towards the spring season, it is better to keep the lower value of inclination angle β.

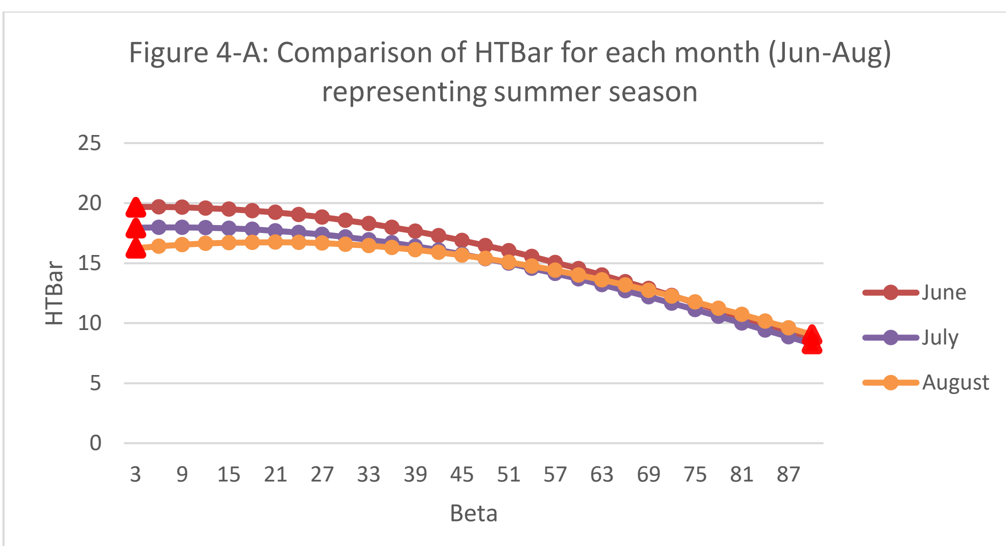

Figure 4-A: Comparison of $\overline{H_T}$ for each month (Jun-Aug) representing summer season

There are three lines on the graph, each representing a different month of the summer season: June, July, and August. The lines show how $\overline{H_T}$ changes as the inclination angle β increases for each of these months. All three lines show a downward trend, which means that as inclination angle β increases, $\overline{H_T}$ decreases. This suggests that $\overline{H_T}$ is highest in June and decreases over the course of the summer. We can also observe a negative corelation betweeen the values of month and inclination angle β.

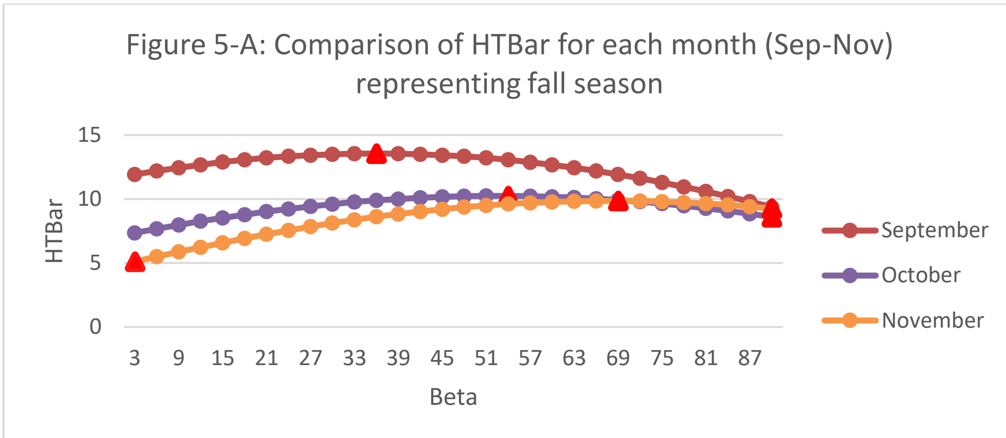

Figure 5-A: Comparison of $\overline{H_T}$ for each month (Sep-Nov) representing fall season

The graph illustrates how $\overline{H_T}$ changes as inclination angle β increases for each of these months. All three lines except for November show a downward trend, indicating that as inclination angle β increases, $\overline{H_T}$ decreases. In November, the value of $\overline{H_T}$ was minimum amongst all but as the inclination angle β increases, the value of $\overline{H_T}$ also increased. The line for September starts at the highest point on the y-axis and remains the highest throughout, followed by October, and then November. This suggests that $\overline{H_T}$ is highest in September and decreases over the course of the fall.

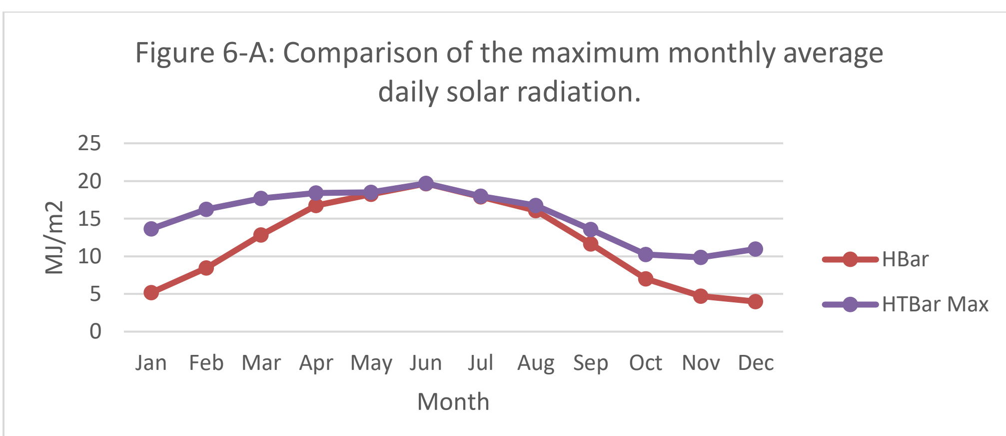

Figure 6-A: Comparison of the maximum monthly average daily solar radiation

Both lines show a seasonal trend with solar radiation starting lower in January, peaking around May through July, and then decreasing towards December. $(\overline{H_T})_{max}$ consistently represents higher values of solar radiation for each month compared to $\overline{H}$ indicating it might be the maximum recorded solar radiation.

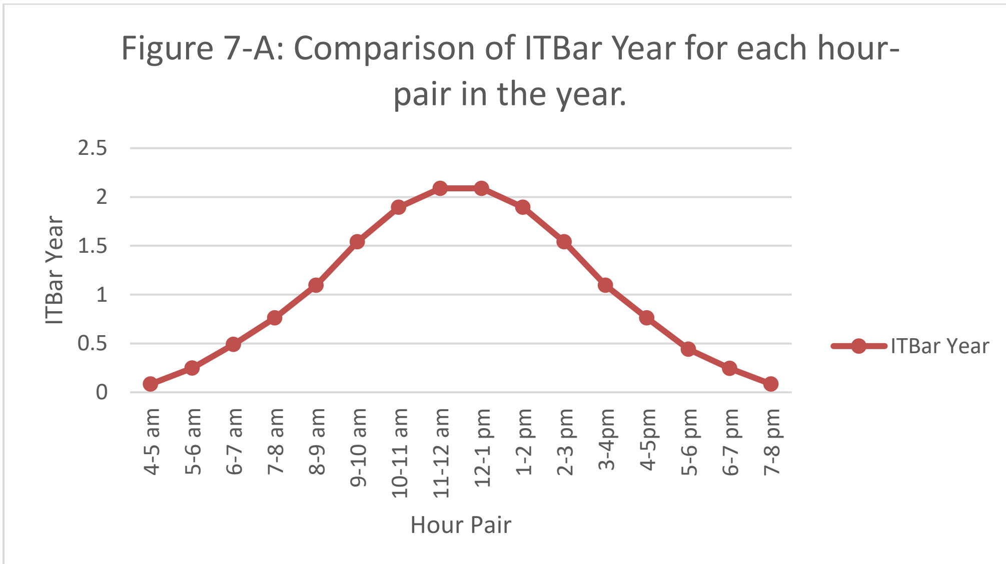

Figure 7-A: Comparison of $(\overline{I_T})$year for each hour pair in the year

The graph displays a bell-shaped curve, which typically suggests a symmetric distribution within the dataset. The curve peaks between 11 am - 12 pm and 12-1 pm, indicating the highest values of $(\overline{I_T})_{\text{year}}$ occur during these hours. The values of $(\overline{I_T})_{\text{year}}$ start low in the early morning (4-5 am), increase to a peak around midday, and then decrease towards the evening (7-8 pm). This pattern could indicate that $(\overline{I_T})_{\text{year}}$ is at its maximum during midday and at its minimum during the early morning and late evening.

Table 5: Results of the estimated values of $(\overline{H_T})max$ at corresponding monthly values of β_{opt}

Month	$(\boldsymbol{\beta_{opt}})_{month}$	$\overline{\boldsymbol{H_O}}$ **(MJ/m²)**	$\bar{\boldsymbol{H}}$ **(MJ/m²)**	$\overline{\boldsymbol{K_T}}$	$\boldsymbol{N}$ **(Hrs)**	$\frac{\overline{\boldsymbol{H_d}}}{\overline{\boldsymbol{H}}}$	$\overline{\boldsymbol{R_b}}$	$\overline{\boldsymbol{H_d}}$ **(MJ/m²)**	$(\overline{\boldsymbol{H_T}})_{max}$ **(MJ/m²)**	$\bar{\boldsymbol{R}}$
January	72	9.96209	5.184	0.520372	8	0.371677	3.628844	1.926775	13.63627	2.630453
February	66	15.50310	8.46	0.545697	10	0.348477	2.444258	2.948117	16.24873	1.920654
March	51	23.23556	12.852	0.553117	12	0.379781	1.632419	4.880955	17.70300	1.377451
April	30	31.97684	16.74	0.523503	12	0.406904	1.188149	6.811577	18.42086	1.100410
May	12	38.69658	18.252	0.471669	14	0.456943	1.031447	8.340125	18.49052	1.013068
June	3	41.64134	19.656	0.472031	16	0.45658	1.002364	8.974541	19.67644	1.001043
July	9	40.15212	17.892	0.445605	14	0.483736	1.013069	8.654997	17.97045	1.004385
August	21	34.56881	16.056	0.464465	14	0.464225	1.102525	7.453601	16.73842	1.042502
September	36	26.3691	11.628	0.440971	12	0.488635	1.397041	5.681852	13.55733	1.165921
October	54	17.74945	7.02	0.395505	10	0.506054	1.397041	3.5525	10.24435	1.45931
November	69	11.24209	4.716	0.419495	8	0.477006	3.248436	2.24956	9.857659	2.090258
December	75	8.538422	3.996	0.468002	8	0.42336	4.122289	1.691746	10.97825	2.747309

This table indicates that $(\overline{H_T})_{max}$ is optimal during the summer season at lower inclination angle while for other seasons we need to adjust the inclination angle to have maximum solar insolation which indirectly affects the efficiency of solar PV systems.

Table 6: Computed results of $(\overline{I_T})_{max}\ \left(\frac{MJ}{m2}\right) at\ \left(\beta_{opt}\right)_{month}$

Month	Hour-pair of the mean day in the month (solar time)															
	4-5 am	5-6 am	6-7 am	7-8 am	8-9 am	9-10 am	10-11 am	11-12 am	12-1 pm	1-2 pm	2-3 pm	3-4 pm	4-5 pm	5-6 pm	6-7 pm	7-8 pm
January					0.8945	1.4427	1.893	2.1464	2.1464	1.893	1.4427	0.8945				
February				0.526	1.0952	1.6701	2.1364	2.3973	2.3973	2.1364	1.6701	1.0952	0.526			
March			0.1672	0.6671	1.2513	1.8237	2.2801	2.5333	2.5333	2.2801	1.8237	1.2513	0.6671	0.1672		
April			0.3756	0.8608	1.3871	1.8808	2.2647	2.4747	2.4747	2.2647	1.8808	1.3871	0.8608	0.3756		
May		0.0049	0.5881	0.997	1.4163	1.7956	2.0837	2.2394	2.2394	2.0837	1.7956	1.4163	0.997	0.5881	0.2299	
June	0.0839	0.374	0.7234	1.1083	1.4931	1.8351	2.092	2.2299	2.2299	2.092	1.8351	1.4931	1.1083	0.7234	0.374	0.0839
July		0.2831	0.6176	0.9932	1.3738	1.7153	1.9735	2.1126	2.1126	1.9735	1.7153	1.3738	0.9932	0.6176	0.2831	
August		0.0881	0.4302	0.8404	1.2748	1.6763	1.9855	2.1539	2.1539	1.9855	1.6763	1.2748	0.8404	0.4302	0.0881	
September			0.1822	0.5561	0.9837	1.3976	1.7254	1.9066	1.9066	1.7254	1.3976	0.9837	0.5561	0.1822		
October				0.3012	0.6734	1.0521	1.3605	1.5333	1.5333	1.3605	1.0521	0.6734	0.3012			
November					0.6083	1.0212	1.3616	1.5536	1.5536	1.3616	1.0212	0.6083				
December					0.6942	1.1714	1.5653	1.7875	1.7875	1.5653	1.1714	0.6942				
$(\overline{I_T})_{year}$	0.0839	0.2484	0.4884	0.7611	1.0955	1.5402	1.8935	2.0890	2.0890	1.8935	1.5402	1.0955	0.7611	0.4406	0.2438	0.0839
$\left(\beta_{opt}\right)_{year}$	41.5^{o}															

This table indicates that $(\overline{I_T})_{year}$ is at its maximum during midday and at its minimum during the early morning and late evening.

Part B:

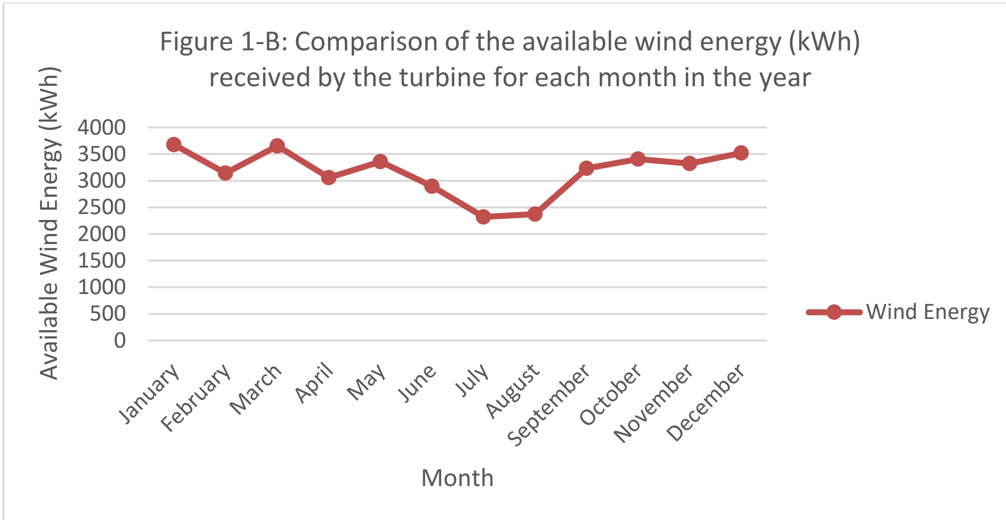

Figure 1-B: Comparison of the available wind energy (kWh) received by the turbine for each month in the year

The graph illustrates the variability of wind energy available to a turbine throughout the year. There is a noticeable decrease in wind energy during the middle months, particularly from June to August, while the rest of the year shows relatively stable energy generation. During the summer months, wind speed decreases compared to other months, likely due to higher temperatures that reduce air density, thereby lowering overall wind energy generation. In contrast, January and December show higher wind energy availability, indicating more favourable wind conditions for power generation during these periods.

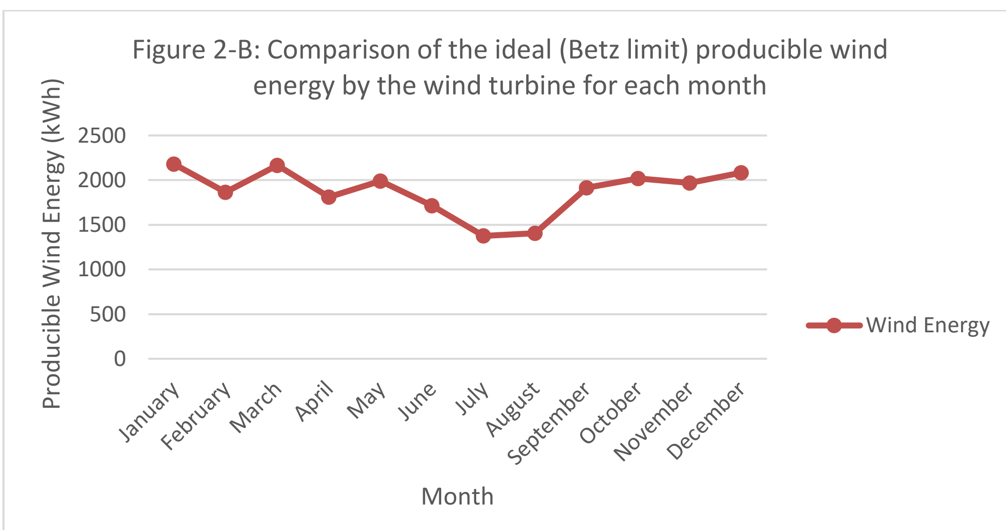

Figure 2-B: Comparison of the ideal (Betz limit) producible wind energy by the wind turbine for each month

The graph is similar to the previous one, but the values are adjusted to reflect the Betz limit, which represents the maximum efficiency achievable by a wind turbine. Consequently, the values are reduced compared to the available wind energy, illustrating the realistic energy output considering the Betz limit constraints.

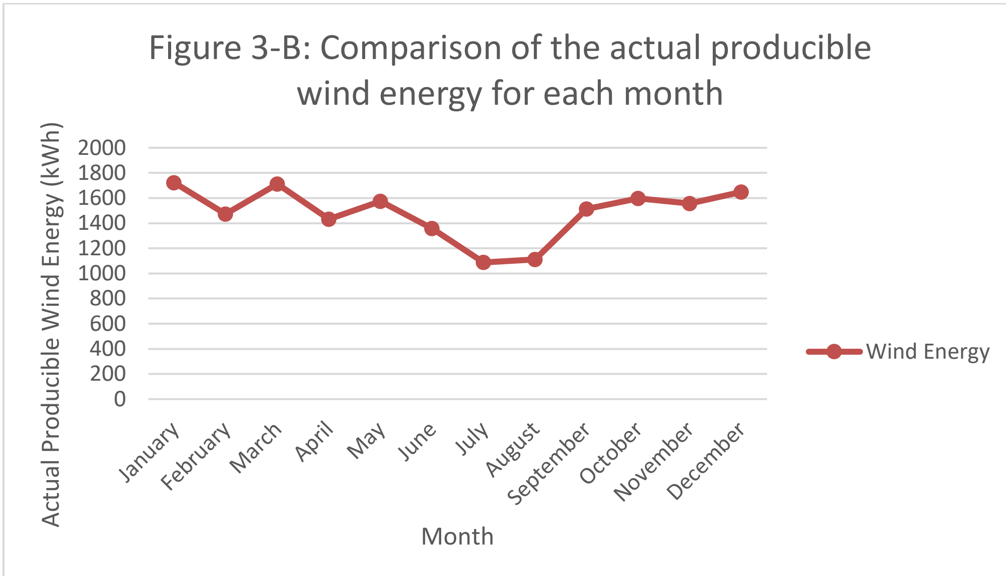

Figure 3-B: Comparison of the actual producible wind energy for each month

The graph is similar to the previous one but adjusted to reflect the actual efficiency achievable by the wind turbine. Considering the actual efficiency (η_{act}) as 0.4687, calculated from Figure k-1[1] using a two-blade high-speed wind turbine by plotting the graph in Excel and deriving the function, this graph was obtained for actual producible wind energy. We can observe a reduction in the values of wind energy compared to the available wind energy, reflecting the realistic output given by the turbine's actual efficiency.

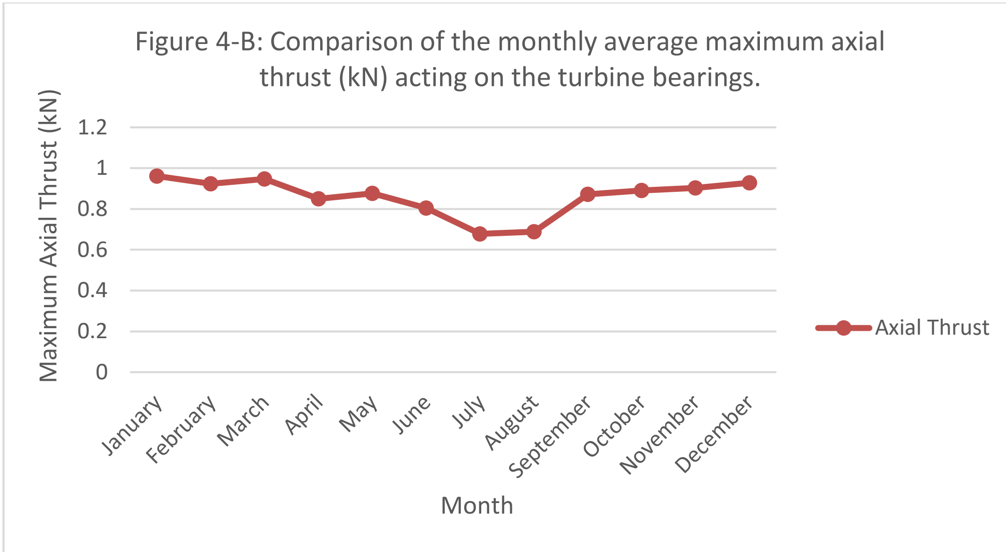

Figure 4-B: Comparison of the monthly average maximum axial thrust (kN) acting on the turbine bearings.

The axial thrust on the turbine bearings remains relatively constant throughout the year, with minor fluctuations around a value just below 1 kN. This consistency in axial thrust suggests that the bearings experience a steady load, which is beneficial for predicting maintenance schedules and bearing lifespan. The graph indicates that the turbine is designed to handle the axial load efficiently, as there are no significant spikes or drops in thrust levels. The stable axial thrust values imply that the turbine can operate reliably without unexpected stresses on the bearings, which is crucial for long-term operation.

Conclusion

This study has provided a comprehensive analysis of optimizing solar photovoltaic (PV) panel performance and assessing wind energy potential for a specified site. Through meticulous calculations and simulations, the following conclusions have been drawn:

The determination of the unique optimum tilt angle (β_{opt}) for a solar PV panel is crucial for maximizing the incident solar radiation on the collector surface throughout the year. By identifying the optimum tilt angle for each month, the PV panels can be adjusted to capture the maximum amount of solar energy, thereby enhancing the overall efficiency of the solar energy system. This monthly optimization ensures that the PV system adapts to the seasonal variations in the sun's position, leading to significant improvements in energy capture and utilization. Consequently, this tailored approach minimizes the PV array area required to meet a specific energy demand, reducing both the cost and spatial footprint of the solar installation.

The second component of this study evaluated the feasibility of installing a horizontal-axis, two-blade, high-speed wind turbine by analyzing monthly wind speed data and energy density. The findings showed sufficient wind resources at the site, justifying the turbine installation. The study adjusted the theoretical maximum energy output using the Betz limit and identified a suitable commercial turbine model. Analysis of axial thrust revealed a consistent load, indicating efficient turbine design and predictable maintenance, crucial for long-term operational efficiency and component lifespan.

The combined findings from the solar PV and wind energy analyses provide a holistic understanding of the renewable energy potential at the specified site. By optimizing the solar PV system and evaluating the feasibility of wind turbine installation, this study contributes to a balanced and efficient renewable energy portfolio. The integration of these two energy sources can significantly enhance the site's overall energy output, reduce dependence on non-renewable energy sources, and promote sustainable energy practices.

References

[1] Dr. Basel Ismail, EMEC-5671-SB: Renewable Energy for Mechanical Engineering Systems, 2024.

[2] Wind Turbine Reference Link - https://eocycle.com/s-series/

[3] Location Information - https://en.wikipedia.org/wiki/Alma,_Quebec